


8519

NACA TN 2093

TECH LIBRARY KAFB, NM  
 0065395



# NATIONAL ADVISORY COMMITTEE FOR AERONAUTICS

TECHNICAL NOTE 2093

FORMULAS AND CHARTS FOR THE SUPERSONIC LIFT AND DRAG OF  
 FLAT SWEPT-BACK WINGS WITH INTERACTING  
 LEADING AND TRAILING EDGES

By Doris Cohen

Ames Aeronautical Laboratory  
 Moffett Field, Calif.



Washington

May 1950

TECHNICAL NOTE  
 2093

319.98 191



---

**TECHNICAL NOTE 2093**

---

**FORMULAS AND CHARTS FOR THE SUPERSONIC LIFT AND DRAG OF  
FLAT SWEPT-BACK WINGS WITH INTERACTING  
LEADING AND TRAILING EDGES**

By Doris Cohen

**SUMMARY**

The problem is considered of a wing with rectilinear plan form swept so that both leading and trailing edges lie within their respective Mach cones; moreover, the Mach lines from the trailing-edge apex intersect the leading edge. Formulas and design charts are presented for the lift in such a case, based on approximate formulas for the lift distribution developed in NACA TN 1991, 1949. The charts cover a practical range of aspect ratios and plan forms of moderate taper, with tips parallel to the stream. The leading-edge thrust and drag due to lift are also readily calculated from the material presented. Numerical results and an application of the charts are included.

**INTRODUCTION****Range of Applicability of Formulas**

Problems in linearized supersonic wing theory are characterized primarily by the orientation relative to the wing boundaries of the Mach lines arising from the various points of disturbance defining those boundaries. Therefore, even when the plan form of a wing is specified, a series of problems arises if the wing is to fly through any considerable range of Mach numbers.

Paradoxically, the problem of the flow at higher Mach numbers has proved more readily amenable to solution than that at lower speeds, because at the higher speeds the zones of influence (Mach cones) are narrow and interference problems are fewer. In the case of the conventional swept-back wing at an angle of attack, four Mach number ranges may be said to have been investigated to a sufficient extent that the lift and drag of any specified wing is readily obtainable. The aerodynamic characteristics were first computed (reference 1) for that range of Mach

numbers in which only the center sections of the wing are included in the Mach cone from the leading-edge apex; formulas have also been given (reference 2) for the next lower range, where the leading-edge Mach line cuts the tip; formulas (reference 2) and charts (reference 3) have been given for a third range, where the leading-edge Mach line stands ahead of the wing, but the Mach line from the trailing-edge apex is behind the wing; and formulas have been given (reference 2) for the fourth case, in which the trailing-edge Mach cone includes part of the tip, but not the leading edge.

The last of these cases is illustrated in figure 1(a). In figure 1(b), the same wing is shown at a smaller Mach number such that the trailing-edge Mach line now intersects the leading edge. In reference 4, the flow in such a case was investigated and formulas for the load distribution were derived. In the present report, the load distribution will be integrated to obtain formulas for the total lift. Formulas for the leading-edge thrust and the drag due to lift will also be presented.

The Mach number range to which the formulas and charts apply is indicated as a function of taper ratio  $\lambda$  and aspect ratio  $A$  for several angles of sweepback  $\Lambda$  in figure 2. The upper-limit curves are determined by the condition that the trailing-edge Mach line intersects the wing tip at the leading edge. Above these curves, the formulas of reference 2 may be used. A lower Mach number range, merging into the transonic and such that the flow field of one wing tip extends laterally to include a part of the other tip, is defined by the lower-limit curves. The flow pattern in such a case is too complicated to be treated by the method of the present report. Mach numbers low enough to permit wing-tip interference fall within the scope of the approximate theory of reference 5.

The problem of wing-tip interaction also, of course, sets a lower limit on the range of aspect ratios covered. On the other hand, the method of reference 4 and the present paper may in theory be applied to the complete range of aspect ratios to the right of the boundaries shown in figure 2. However, the necessary formulas have been developed only up to a certain point beyond which the services of high-speed computing machinery would be required for their evaluation. Both mathematical and physical considerations make the application of the method to very highly tapered plan forms inadvisable. For cases of moderate taper and a practical range of aspect ratios, charts have been computed to facilitate the calculation of both lift and drag due to lift. The formulas and charts have been developed for wings with tips parallel to the stream only, but the general procedure is applicable to wings with raked tips also.

The symbols used are listed in the appendix.

## General Outline of the Procedure

In reference 4 it was found that, when interaction takes place between the flow fields of the leading and trailing edges, the wing plan form appears to comprise two principal regions, separated (fig. 1(b)) by the Mach line arising at the point of intersection of the trailing-edge Mach line and the leading edge. Ahead of this line (region I) the flow is most readily described in terms of conical fields. Behind this line (region II), the flow is more nearly two-dimensional, and the loading can be approximated by the well-known subsonic flat-plate formula, corrected in magnitude to give the proper value of the pressure at the leading edge of each section. The formulas for correcting the two-dimensional loading are given in reference 4. For an infinitely long wing, of course, the loading approaches the subsonic flat-plate loading, corrected for the angle of yaw according to simple sweep theory.

The total lift is found using for the loading in region I the conical-flow solutions of reference 2 and in region II the formulas given in reference 4. From the integrated lift and the leading-edge thrust, the drag due to lift can be calculated. The leading-edge thrust in region I is the same as that for the triangular wing with the same leading-edge sweep, and has been given by Jones (reference 6), Hayes (reference 7), Robinson (cited in reference 8), and others. The disturbance arising at the trailing edge affects the leading-edge suction in region II. Formulas are derived for calculating the resulting thrust, from which the drag due to lift follows.

## FORMULAS FOR LIFT

## Region I

Conical-flows method.— The term "conical-flows method" is used to designate briefly a method of superposition of conical flow fields<sup>1</sup> developed by Lagerstrom (reference 9) as an extension of some earlier work by Busemann (reference 10). Thus, the load distribution on a swept-back wing is calculated by superposing on the conical loading of an infinite triangular plate other conical flow fields of such magnitude and orientation as to cancel loading on the portions of the triangular plate lying outside the boundaries of the specified swept-back wing. This process, as applied at the trailing edge of a swept-back wing, is more fully described in reference 2.

---

<sup>1</sup>A conical field is one in which the velocities are constant along rays emanating from a point (the apex of the cone).

---

In figure 1(b), region I has been further divided into regions Ia and Ib by the Mach line from the trailing-edge apex. Region Ib is the region in which the loading is modified by the addition of the fields used to cancel the load behind the trailing edge. In region Ia, the loading is simply that on a triangular wing having the same apex angle as the swept-back wing.

The conical flow fields were originally derived most conveniently as velocity, rather than pressure, fields. The loading is obtained from the velocity by the linearized relation

$$\frac{\Delta p}{q} = \frac{\Delta u}{V}$$

where  $u$  is the streamwise component of the perturbation velocity on the upper surface,  $V$  is the stream velocity, and  $\Delta p/q$  is the coefficient of lifting pressure.

Load distribution in region I.— In terms of the conical variable  $a = \beta y/x$ , the loading over the triangular wing is given by

$$u_{\Delta} = \frac{m u_0}{\sqrt{m^2 - a^2}} \quad (1)$$

where

$$u_0 = \frac{m V \alpha}{\beta R (\sqrt{1 - m^2})} \quad (2)$$

is the streamwise component of the perturbation velocity along the wing center line ( $a=0$ ) and  $u_{\Delta}$  is the same velocity component elsewhere on the wing.

Cancellation of the load in the wake, as described in reference 2, is accomplished by superposing first a symmetrical field having a constant-load region coincident with the wake to cancel the perturbation velocity  $u_0$  throughout the wake, and then an infinite number of infinitesimally loaded oblique elements to cancel the remaining lift. Figure 3 shows the constant-load region (shaded) of a single "oblique" flow field.

Cancellation of  $u_0$  induces on the wing a pressure distribution (equation (51) of reference 2, corrected) proportional to

$$(\Delta u)_0 = - \frac{u_0}{K(\sqrt{1 - m_t^2})} F(\sqrt{1 - m_t^2}, \phi) \quad (3)$$

where  $K(\sqrt{1-m_t^2})$  is the complete elliptic integral of the first kind of modulus  $\sqrt{1-m_t^2}$ , and  $F$  is the incomplete integral with argument

$$\phi = \sin^{-1} \sqrt{\frac{1-t_o^2}{1-m_t^2}} \quad (4)$$

Each of the oblique elements induces on the wing the perturbation velocity (equation (50) of reference 2)

$$(\Delta u)_a = \frac{-u_a}{\pi} \cos^{-1} \frac{(1-a)(t_a-m_t)-(m_t-a)(1-t_a)}{(1-m_t)(t_a-a)} \quad (5)$$

where  $u_a$  is the differential of  $u_\Delta$  obtained by differentiating with respect to  $a$ , or

$$u_a = \frac{m_0 a}{(m^2-a^2)^{3/2}} da \quad (6)$$

Uncorrected lift in region I.— In order to obtain the total lift in region I,<sup>2</sup> we first integrate the uncorrected loading of the triangular wing over the entire area, obtaining

$$\frac{L_Q}{q\alpha} = \frac{4m}{\beta} \frac{u_0}{V\alpha} c_0^2 \left\{ \frac{1+m}{(1-m)^3} \left[ \frac{1}{\sqrt{1-m^2}} \cos^{-1} \frac{m^2+a_2}{m(1+a_2)} - \frac{\sqrt{m^2-a_2^2}}{1+a_2} \right] + \frac{m_t^2}{m_t^2-m^2} \left( \frac{m}{m_t} - \frac{\sqrt{m^2-a_2^2}}{m_t-a_2} \right) + \left( \frac{m_t}{\sqrt{m_t^2-m^2}} \right)^3 \left[ \cos^{-1} \frac{m^2-m_t a_2}{m(m_t-a_2)} - \cos^{-1} \frac{m}{m_t} \right] \right\} \quad (7)$$

where  $a_2$  is the value of  $a$  corresponding to the ray through the point of intersection  $x_2, y_2$  of the trailing edge and the Mach line separating regions I and II. (See figs. 1 and 3.) In terms of the wing plan-form parameters,

$$a_2 = \frac{2mm_t}{1+m+m_t-mm_t} \quad (8)$$

---

<sup>2</sup>Formulas which follow are for the complete wing; that is, the left-hand side is included.

When  $m_t = m$  (untapered wing), the second part of equation (7) becomes indeterminate. In this case,

$$\frac{L_Q}{q\alpha} = \frac{4m}{\beta} \frac{u_0}{V\alpha} c_0^2 \left\{ \frac{1+m}{(1-m)^3} \left[ \frac{1}{\sqrt{1-m^2}} \cos^{-1} \frac{m^2+a_2}{m(1+a_2)} - \frac{\sqrt{m^2-a_2^2}}{1+a_2} \right] + \frac{1}{3} \left[ \left( 1 + \frac{m}{m-a_2} \right) \sqrt{\frac{m+a_2}{m-a_2}} - 2 \right] \right\} \quad (9)$$

Wake corrections.— The wake corrections are to be integrated over region Ib. Integration of the symmetrical wake correction (equation (3)) yields

$$\frac{(\Delta L)_Q}{q\alpha} = \frac{-16m^2 x_1^2}{\beta(1+m_t)} \frac{u_0}{V\alpha} \left\{ 1 - \frac{2}{1-m_t} \left[ 1 - \frac{E(\sqrt{1-m_t^2})}{K(\sqrt{1-m_t^2})} \right] \right\} \quad (10)$$

where

$$x_1 = \frac{c_0}{1-m} \quad (11)$$

is the  $x$  coordinate of the intersection of the trailing-edge Mach line with the leading edge. (See fig. 3.)

For each oblique element, the reduction in lift is given by

$$\frac{1}{q\alpha} \frac{d\Delta L}{da} da = - \frac{2u_a}{\beta V\alpha} \frac{1+m_t}{1+a} (m_t-a)(x_2-x_a)^2 \left[ \sqrt{\frac{(1+m_t)(1-a)}{2(m_t-a)}} - 1 \right] \quad (12)$$

in which

$$x_2 = \left( \frac{1+m}{1-m} + m_t \right) \frac{c_0}{1+m_t} \quad (13)$$

is the  $x$  coordinate of the intersection of the Mach line from  $x_1, y_1$  with the trailing edge (see fig. 3) and

$$x_a = \frac{m_t c_0}{m_t - a} \quad (14)$$

is the  $x$  coordinate of the apex of the element  $a$ .

Lift in region I.— The total lift in region I is then given by

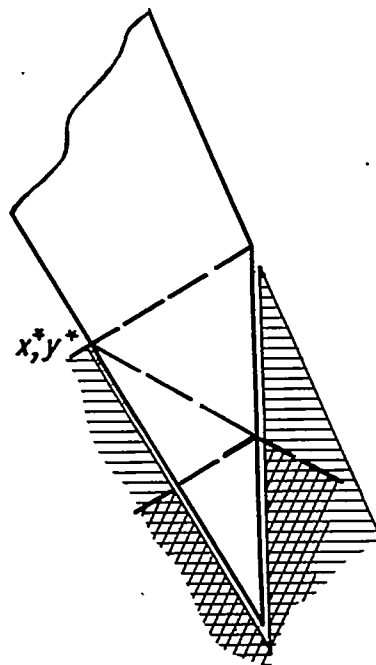
$$\left(\frac{L}{q\alpha}\right)_I = \frac{L_0}{q\alpha} + \frac{(\Delta L)_0}{q\alpha} + \frac{2}{q\alpha} \int_0^{a_2} \frac{d\Delta L}{da} da \quad (15)$$

The quantity  $\frac{\beta^2}{m^2 c_0^2} \left(\frac{L}{q\alpha}\right)_I$  is plotted against  $m_t$  in figure 4 for

several values of the ratio  $m/m_t$ . This latter parameter is the ratio of the tangents of the semiapex angles of the leading and trailing edges and is constant for any one wing through the Mach number range.

### Region II

Tip-effect problems.— In figure 1(b), region II is shown divided into two sections by the Mach line from the leading edge of the tip. Such a division is actually an oversimplification of the problem. While region IIa can be treated, by the method of reference 4, in such a way as automatically to satisfy the Kutta condition at the trailing edge, the tip effect, which modifies the lift in region IIb, has not been determined so as to take this condition into account. In the cancellation method used to determine the tip effect, a so-called "primary tip correction" is first obtained by superposing conical flows to reduce the lift to zero along and outboard of the side edge. A further succession of steps (reference 2) is required to cancel lift introduced in the wake behind region IIb, and thereafter outboard of the tip within the Mach cone from  $x^*, y^*$  (see sketch) and so on. The corrections obtained by this procedure alternate in sign and become successively smaller in magnitude, while increasing in mathematical complexity. Since, moreover, it is known from experiments that the assumed flow in the tip regions is at variance with the physical flow, it would be illogical to attempt any precise evaluation of these corrections. A simple formula will therefore be given, following the derivation of the primary tip correction, for obtaining a fair estimate of the "secondary correction"; further corrections will be neglected.



Loading in region II.— Except for tip losses, the lift in region II may be



calculated by integrating out to the tip the approximate load distribution given in reference 4. This loading is

$$\frac{\Delta p}{q\alpha} = 4\sigma \sqrt{\frac{[\beta y - m_t(x - c_o)]c_o}{[mx - m_t(x - c_o)](mx - \beta y)}} \quad (16)$$

which is merely the subsonic two-dimensional flat-plate loading, applied on sections taken normal to the stream, and with a correction factor inserted to bring the loading at the leading edge into agreement with that derived for the swept-back wing by the conical-flows method. The theoretical loading at a subsonic leading edge is, of course, infinite in any case, with the infinity entering as the reciprocal square root of the distance to the leading edge. The coefficient  $\sigma$  is a measure of the strength of the leading-edge singularity in the loading on the swept-back wing.

It is most convenient to describe the leading-edge singularity in terms of the coefficient in the perturbation velocity  $u$  of  $(mx - \beta y)^{-1/2}$ , where the quantity  $(mx - \beta y)$  is  $\beta$  times the spanwise distance to the leading edge. This coefficient is then  $u\sqrt{mx - \beta y}$  and the strength of the singularity in  $u$  is the limit of its value as  $\beta y$  approaches  $mx$  (the leading edge). The coefficient  $\sigma$  is a nondimensional form of the same quantity:

$$\sigma = \left( \frac{u}{V\alpha} \sqrt{\frac{mx - \beta y}{c_o}} \right)_{\beta y = mx} \quad (17)$$

and is a function of  $x$ .

In line with the general procedure of the conical-flows method, the coefficient  $C_{\Delta}$  of  $(mx - \beta y)^{-1/2}$  corresponding to the triangular-wing velocity distribution is found first, and is then corrected to take account of the effects of canceling the loading in the wake, by the symmetrical canceling element and by the oblique elements. The resulting expression for  $\sigma$  is

$$\sigma(x) = \frac{1}{V\alpha\sqrt{c_o}} \left[ C_{\Delta} + (\Delta C)_o + \int_0^{a_o} \frac{d\Delta C}{da} da \right] \quad (18)$$

where

$$C_{\Delta} = u_o \sqrt{\frac{mx}{2}} \quad (19)$$

is the uncorrected (i.e., triangular-wing) coefficient;

$$(\Delta C)_0 = \frac{-4m_0}{\pi m_t K(\sqrt{1-m_t^2})} \sqrt{\frac{mx}{1+m}} \left[ K(k)E(k,\psi) - E(k)F(k,\psi) \right] \quad (20)$$

with  $k = \sqrt{\frac{2m_t(1-\tau_0)}{(1-m_t)(\tau_0+m_t)}}$ ,  $\psi = \sin^{-1} \sqrt{\frac{\tau_0+m_t}{2\tau_0}}$ , and  $\tau_0 = \frac{mx}{x-c_0}$

is the symmetrical wake correction; and

$$\frac{d\Delta C}{da} da = \frac{-4m}{\pi^2 \sqrt{1+m}} \frac{u_a}{a} \sqrt{1-a} \sqrt{(m_t-a)x-m_t c_0} \left\{ \sqrt{\frac{(1+a)(\tau_a-a)}{(1-a)(m_t-a)}} \left[ K(k_a)E(k_a,\psi_a) - E(k_a)F(k_a,\psi_a) \right] - \sqrt{\frac{\tau_a}{m_t}} \left[ K(k_a)E(k_a,\psi_0) - E(k_a)F(k_a,\psi_0) \right] \right\} \quad (21)$$

is the correction for a single oblique wake element, with

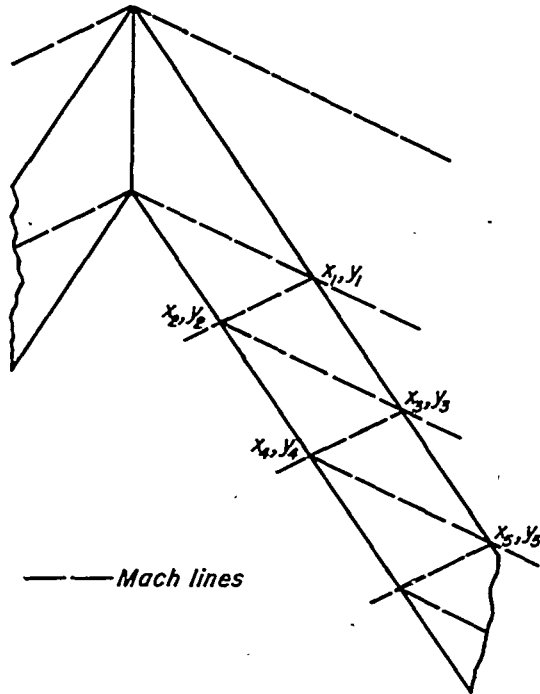
$$\tau_a = \frac{(m_t-a)mx-m_t c_0 a}{(m_t-a)x-m_t c_0} \quad \psi_a = \sin^{-1} \sqrt{\frac{(m_t-a)(1+\tau_a)}{(\tau_a-a)(1+m_t)}}$$

$$k_a = \sqrt{\frac{(1+m_t)(1-\tau_a)}{(1-m_t)(1+\tau_a)}} \quad \psi_0 = \sin^{-1} \sqrt{\frac{m_t(1+\tau_a)}{\tau_a(1+m_t)}}$$

The upper limit of integration is

$$a_0 = m_t \frac{(1-m)x-c_0}{(1-m)x-m_t c_0} \quad (22)$$

Equation (18) for the coefficient of the leading-edge singularity is mathematically complete for points immediately beyond  $x_1, y_1$  along the leading edge, but if the aspect ratio is very high or the Mach number very low, the Mach line from  $x_2, y_2$  may intersect the leading edge



(see sketch) and bring about further modifications of the flow on the outboard portions of the wing. The only effect of this modification on the formulas presented herein is the introduction of additional terms into the expression for  $\sigma$  for values of  $x$  beyond  $x_3$ , and in still more extreme cases, beyond  $x_5$ , and so on. Evaluation of these terms by the conical-flows method involves multiple integration and is impractical except with the aid of high-speed computing machinery. Each successive correction (to  $\sigma$ ) is initially zero and enters with zero slope at  $x_3$ , zero slope and curvature at  $x_5$  and so on, so that the three-term expression for  $\sigma$  given by equation (18) may be used with satisfactory accuracy for some distance beyond the last value of  $x$  ( $x_3$ ) for which it is strictly valid. In practice, the third term in equation (18) may also be neglected for values of  $x$  only slightly greater than  $x_1$ .

Charts giving  $\frac{\beta\sigma}{m} \sqrt{\frac{1-m}{m}}$  as a function of  $\frac{x-x_1}{c_0}$  for the values of the taper-ratio parameter  $\frac{m}{m_t}$  covered in figure 4 are presented in figure 5 as an aid to computing. The curves were computed using equation (18) and are therefore exact only up to  $x=x_3$  (shown by a vertical mark in each curve). The points  $x=x_5$  are also indicated (by x's) as a more practical limit to which use of the curves may be extended. (These points are off the scale for  $m_t = 0.8$  and  $0.9$  in figure 5(a)). When the wings are untapered ( $m/m_t = 1.0$ ), asymptotes

$$\frac{\beta\sigma}{m} \sqrt{\frac{1-m}{m}} = \frac{1}{\sqrt{1+m}}$$

derived from simple sweep theory, may be drawn. The relative positions of the curves in figure 5(a) and their asymptotes suggest that a further extension beyond  $x_5$  will probably not introduce any serious error in these cases.

The curves are for the most part regular enough to permit interpolation within intervals of 0.2 of  $m_t$ . However, at  $m_t = 1.0$  the lines

diminish to a point on the vertical axis; a curve for  $m_t = 0.9$  was therefore inserted in the charts for moderate values of  $m/m_t$ . With  $m/m_t$  less than 0.5,  $m_t = 0.9$  represents, if  $x > x_1$ , such extreme taper that the successive points of reflection of the Mach lines ( $x_3, x_5, \dots$ ) take place within a very small fraction of a chord-length and no useful curve can be drawn. No curves are drawn for  $m_t$  smaller than 0.2 because of the tip-interference limitation discussed in the introduction.

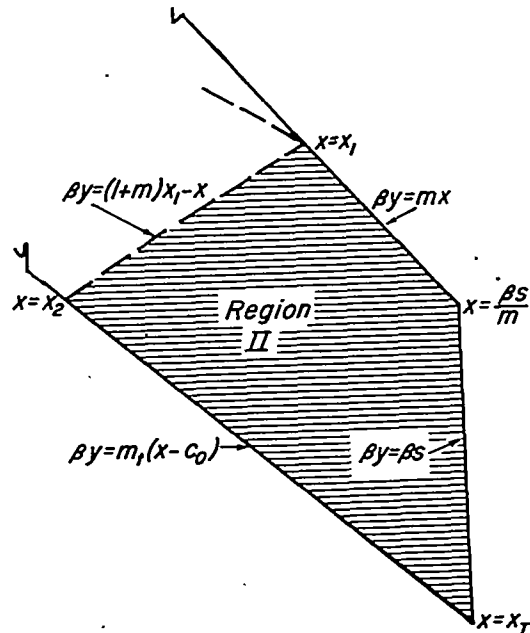
Uncorrected lift, region II.— In order to find the total lift (except for tip losses) in region II, a double integration with respect to  $x$  and  $y$  is performed on equation (16). A first integration, with respect to  $y$ , yields for the indefinite integral

$$\beta \int \frac{\Delta p}{\rho a} dy = 4\sigma(x) \sqrt{c_0} \left[ \sqrt{\frac{(mx-\beta y)(m_t c_0 - m_t x + \beta y)}{m_t c_0 - (m_t - m)x}} + \sqrt{m_t c_0 - (m_t - m)x} \tan^{-1} \sqrt{\frac{mx - \beta y}{m_t c_0 - m_t x + \beta y}} \right] \quad (23)$$

The values of  $\beta y$  to be substituted as limits in equation (23) are indicated in the sketch to the right. Along the leading edge, the right-hand member of equation (23) reduces to zero; along the trailing edge it becomes

$$2\pi \sigma(x) \sqrt{c_0} \sqrt{m_t c_0 - (m_t - m)x} \quad (24)$$

Then the total lift in region II (on both wing halves), except for tip losses, is



$$\left(\frac{L}{q\alpha}\right)_{II} = \frac{8\sqrt{c_0}}{\beta} \left[ \int_{x_1}^{x_2} \sigma(x) \left( f_1 \tan^{-1} \frac{f_2}{f_3} + \frac{f_2 f_3}{f_1} \right) dx + \frac{\pi}{2} \int_{x_2}^{x_T} \sigma(x) f_1 dx - \int_{\frac{\beta s}{m}}^{x_T} \sigma(x) \left( f_1 \tan^{-1} \frac{f_4}{f_5} + \frac{f_4 f_5}{f_1} \right) dx \right] \quad (25)$$

where

$$f_1 = \sqrt{m_t c_0 - (m_t - m)x}$$

$$f_2 = \sqrt{(1+m)(x-x_1)}$$

$$f_4 = \sqrt{m(x-\beta s/m)}$$

$$f_3 = \sqrt{(1+m_t)(x_2-x)}$$

$$f_5 = \sqrt{m_t(x_T-x)}$$

The indicated integrations may be performed numerically or graphically, using values of  $\sigma(x)$  taken from the charts.

Primary tip correction.— A method of approximating the tip-induced reduction in loading is described in reference 4. The uncorrected loading along the tip section is determined by equation (16), simplified by replacing  $\sigma(x)$  by the constant

$$\sigma_s = \sigma \left( \frac{\beta s}{m} \right) \quad (26)$$

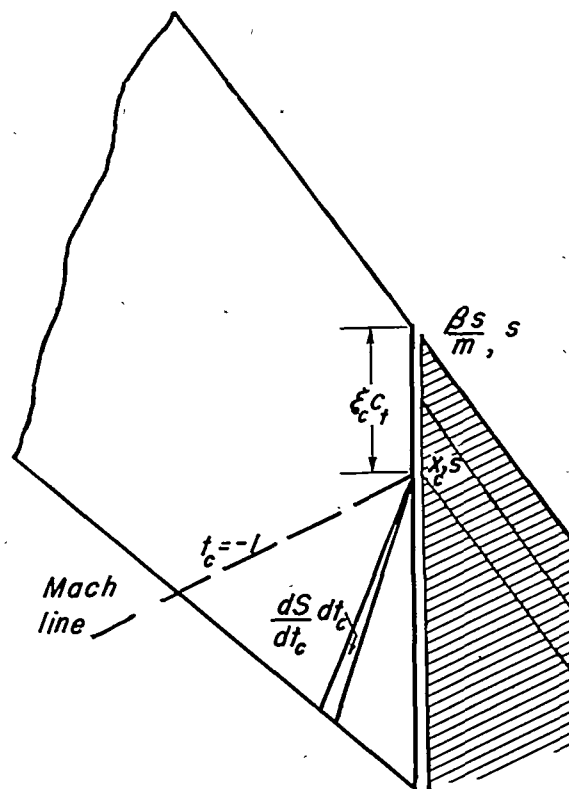
The assumption is then made that the lift to be canceled outboard of the tip is a continuation of this loading along lines parallel to the leading edge of the wing. The cancellation is accomplished by means of the "tip

solutions" of references 2 and 9, flow fields having constant pressure over a region bounded by the tip and a ray extending outward from a point  $x_{c,s}$  on the tip.

In canceling the cylindrical field assumed in this case, the rays would all be parallel to the leading edge. (See sketch.) The streamwise component of velocity on the wing due to one such element is

$$\frac{u_c}{\pi} \cos^{-1} \frac{m+t_c+2mt_c}{t_c-m} \quad (27)$$

where  $u_c$  is the constant value of the streamwise perturbation velocity on the element and  $t_c/\beta$  is the slope of a ray from its apex  $x_{c,s}$ . This velocity is multiplied by  $2\rho V$  to convert to pressure and by



$$\frac{dS}{dt_c} dt_c = \frac{m_t^2 [c_t - (x_c - \frac{\beta s}{m})]^2}{\beta (m_t - t_c)^2} dt_c$$

to obtain the lift on the differential of area shown in the sketch. Then integrating with respect to  $t_c$  from  $-1$  to  $0$  gives the total lift induced on the wing by the single canceling element at  $x_c$ . The result may be written

$$\frac{1}{q\alpha} \frac{d\Delta L}{dx_c} dx_c = \frac{2u_c m_t^2 c_t^2}{\beta V \alpha (m_t - m)} \left( \sqrt{\frac{m+m_t^2}{m_t+m_t^2}} - \frac{m}{m_t} \right) (1-\xi_c)^2 \quad (28)$$

where  $\xi_c$ , as shown in the sketch, is the distance of  $x_{c,s}$  behind the leading edge, divided by the tip chord  $c_t$ , or

$$\xi_c = \frac{x_c - (\beta s/m)}{c_0 + (\beta s/m_t) - (\beta s/m)} \quad (29)$$

Since along the tip, from equation (16),

$$\frac{u(x_c, s)}{V\alpha} = \sigma_s \sqrt{\frac{[\beta s - m_t(x_c - c_0)]c_0}{[m_t c_0 - (m_t - m)x_c](mx_c - \beta s)}}$$

or

$$\frac{u(\xi_c)}{V\alpha} = \frac{\sigma_s}{\sqrt{m\lambda}} \sqrt{\frac{1 - \xi_c}{\xi_c \left(1 - \frac{m_t - m}{m_t} \xi_c\right)}} \quad (30)$$

where  $\lambda$  is the taper ratio  $c_t/c_0$ , the canceling velocities  $u_c$  must be given by the differential

$$\frac{u_c}{V\alpha} = \frac{\sigma_s}{\sqrt{m\lambda}} \frac{d}{d\xi_c} \sqrt{\frac{1 - \xi_c}{\xi_c \left(1 - \frac{m_t - m}{m_t} \xi_c\right)}} d\xi_c \quad (31)$$

Then the primary tip correction to the lift (both tips included)

$$\left(\frac{\Delta_1 L}{q\alpha}\right)_{\text{tip}} = -\frac{4m_t^2 c_t^2}{\beta(m_t - m)} \left(\sqrt{\frac{m+m^2}{m_t+m_t^2}} - \frac{m}{m_t}\right) \frac{\sigma_s}{\sqrt{m\lambda}} \lim_{\xi_c \rightarrow 0} \left[ (1 - \xi_c)^2 \sqrt{\frac{1 - \xi_c}{\xi_c \left(1 - \frac{m_t - m}{m_t} \xi_c\right)}} + \int_{\xi_c}^1 (1 - \xi_c)^2 \frac{d}{d\xi_c} \sqrt{\frac{1 - \xi_c}{\xi_c \left(1 - \frac{m_t - m}{m_t} \xi_c\right)}} d\xi_c \right] \quad (32)$$

which may be integrated by parts to give

$$\left(\frac{\Delta_1 L}{q\alpha}\right)_{\text{tip}} = \frac{-16\sigma_s m_t^2 c_t^2 \sqrt{m}}{3\beta(m_t - m)^3 \sqrt{\lambda}} \left(\sqrt{\frac{m+m^2}{m_t+m_t^2}} - \frac{m}{m_t}\right) \left[ (3m - m_t)K - 2m_t \left(2 - \frac{m_t}{m}\right)E \right] \quad (33a)$$

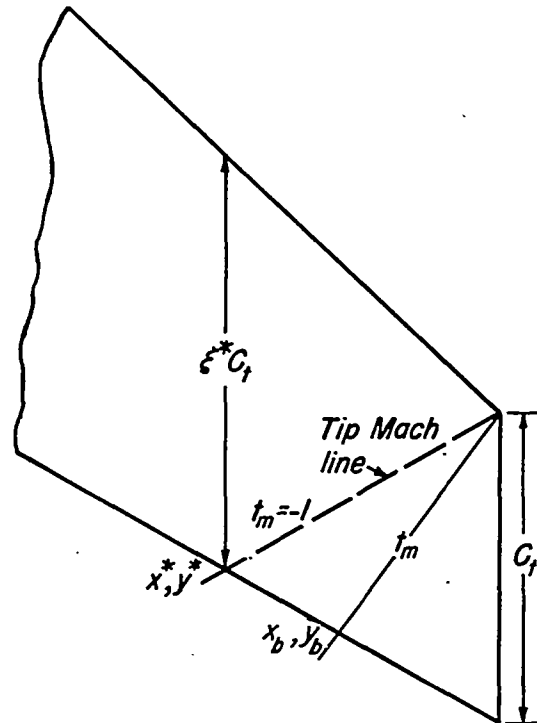
where  $K$  and  $E$  are the complete elliptic integrals of the modulus

$$k = \sqrt{\frac{m_t - m}{m_t}}$$

In the case of an untapered wing, equation (33a) reduces to

$$\left(\frac{\Delta_1 L}{q\alpha}\right)_{\text{tip}} = \frac{-3\pi c_0^2 \sqrt{m}}{2\beta(1+m)} \sigma_s \quad (33b)$$

Secondary tip correction.— The primary tip effect just derived is actually an overcorrection, since the load distribution of which it is the integral does not go to zero at the trailing edge. The residual lift in the wake is the result of superposition of an infinite number of conical fields and therefore cannot be canceled identically in any simple way. Numerical results indicate, however, as pointed out in the previous reports (references 2 and 4), that the major part of the tip effect arises in the cancellation of the infinite pressure at the leading edge. In determining the secondary tip correction to the loading, therefore, it may be assumed as an approximation that the residual velocity field in the wake is conical with respect to the leading-edge tip, the value of the velocity along any ray  $t_m$  (see sketch) being determined by the value at the intersection  $x_b, y_b$  of the ray with the trailing edge. Thus the Kutta condition is satisfied, although some pressure differences remain in the wake.



An expression for the correction to the total lift resulting from this approximate cancellation of the tip-induced velocities at the trailing edge has been given in reference 1 as equation (71), from which may be written



$$\left(\frac{\Delta_2 L}{q\alpha}\right)_{\text{tip}} = -4\beta \left\{ \frac{\Delta u^*}{V\alpha} (s-y^*)^2 \left( \sqrt{\frac{1+m_t}{m_t}} - \sqrt{2} \right) \sqrt{\frac{1+m_t}{m_t}} + \int_{-1}^0 \frac{d(\Delta u/V\alpha)}{dt_m} (s-y_b)^2 \left[ \frac{1}{m_t} + \frac{1}{t_m} \left( \sqrt{\frac{(m_t-t_m)(1-t_m)}{m_t}} - 1 \right) \right] dt_m \right\} \quad (34)$$

where  $x^*, y^*$  (see sketch p. 15) is the point of intersection of the tip Mach line with the trailing edge,  $t_m$  is  $\beta$  times the slope of a ray from the leading-edge tip,  $x_b, y_b$  is the intersection of the ray with the trailing edge,  $\Delta u$  is the velocity to be canceled at  $x_b, y_b$ , and  $\Delta u^*$  is  $\Delta u(x^*, y^*)$ .

Again experience has shown the integral term in equation (34), which involves very lengthy computing, to be considerably smaller than the term in  $\Delta u^*$ . Since only an approximate tip correction is desired, it will suffice, therefore, to calculate

$$\left(\frac{\Delta_2 L}{q\alpha}\right)_{\text{tip}} \cong -4\beta \frac{\Delta u^*}{V\alpha} (s-y^*)^2 \left( \sqrt{\frac{1+m_t}{m_t}} - \sqrt{2} \right) \sqrt{\frac{1+m_t}{m_t}} \quad (35)$$

From reference 4, equation (45),

$$\frac{\Delta u^*}{V\alpha} = \frac{-\sigma_s}{\sqrt{m\lambda\xi^*}} \quad (36)$$

where  $\xi^*$  is the streamwise distance of  $x^*, y^*$  from the leading edge expressed as a fraction of the tip chord; that is,

$$\xi^* = \frac{1}{c_t} \left( x^* - \frac{\beta y^*}{m} \right) \quad (37)$$

It is easily determined that

$$\beta(s-y^*) = \frac{m_t c_t}{1+m_t}$$

and consequently

$$\xi^* = \frac{m_t(1+m)}{m(1+m_t)}$$

With these values, and  $\Delta u^*/V\alpha$  from equation (36), equation (35) becomes

$$\left(\frac{\Delta L}{q\alpha}\right)_{\text{tip}} \cong 4 \frac{\sigma_s}{\beta} \frac{m_t c_t^2}{1+m_t} \frac{1}{\sqrt{(1+m)\lambda}} \left(\sqrt{\frac{1+m_t}{m_t}} - \sqrt{2}\right) \quad (38)$$

Total tip correction.— The total tip correction, to the degree of approximation discussed, is the algebraic sum of equations (33) and (38). Except for the occurrence of  $\sigma_s, c_t$  and  $\lambda$  in the coefficient, the resultant expression is a function of  $m$  and  $m_t$  only, independent of

the tip location. Values of  $\frac{\beta\sqrt{\lambda}}{\sigma_s c_t^2} \left(\frac{\Delta L}{q\alpha}\right)_{\text{tip}}$  have been plotted in figure 6, in a form similar to the chart of  $\left(\frac{L}{q\alpha}\right)_I$  (fig. 4).

#### Numerical Example

As a summary of the method, a sample calculation will be outlined. The lift-curve slope  $C_{L\alpha}$  will be calculated for an untapered wing of 10-foot chord and 40-foot span, swept back  $45^\circ$  and flying at a Mach number of 1.08. Then  $\cot \Lambda = 1.0$ ,  $\beta = 0.4$ ,  $m = 0.4$ ,  $m_t = 0.4$  and, from figure 4,

$$\left(\frac{L}{q\alpha}\right)_I = 13.30 \frac{m^2}{\beta^2} c_o^2 = 1330 \text{ square feet}$$

(It should be noted that  $\frac{m}{\beta} = \cot \Lambda$ )

With values of  $\sigma$  obtained from figure 5(a), graphical integration of equation (25) gives

$$\left(\frac{L}{q\alpha}\right)_{II} = 531 \text{ square feet}$$

Since the leading-edge sweep is  $45^\circ$ , the tip is at  $x = 20$ , and, from

figure 5(a),  $\sigma_s = 0.635 \left(\frac{m}{\beta}\right) \sqrt{\frac{m}{1-m}} = 0.518$ . From figure 6, since  $\lambda = 1$ ,

$$\left(\frac{\Delta L}{q\alpha}\right)_{\text{tip}} = -1.69 \frac{c_t^2 \sigma_s}{\beta} = -219 \text{ square feet}$$

Combining the three components of the lift, we obtain  $\frac{L}{q\alpha} = 164.2$  square feet and

$$C_{L\alpha} = \frac{1}{S} \left( \frac{L}{q\alpha} \right) = 4.10$$

#### DRAG DUE TO LIFT

The drag due to lift can be found as the integral around the airfoil of the incremental pressure  $\rho uV$  times the slope  $w/V$  of the surface. In the case of a thin flat airfoil, this calculation gives merely the lift times the angle of attack over most of the surface. However, as is discussed in reference 11 in connection with the two-dimensional wing in subsonic flow, an infinite pressure acting on the leading edge results in a suction force, which tends to reduce the total drag. When the wing is swept behind the Mach lines from its apex, a similar suction can exist in supersonic flow, since the pressure on a subsonic leading edge is theoretically infinite.

Hayes (references 7 and 12), Robinson (see reference 8), and others have derived the formula for the suction force on a subsonic leading edge by assuming the flow near the leading edge to be essentially two-dimensional and applying the results of two-dimensional potential theory. The simple result obtained in that manner has been verified for the long swept-back wing by application of the somewhat different approach of reference 13.

By the two-dimensional approach, the suction force is found to be proportional to the square of the strength of the leading-edge singularity in the perturbation velocity  $u$ . This quantity has already been discussed in connection with the lift in region II, where the strength of the leading-edge singularity was defined as the coefficient of the inverse square root of  $mx - \beta y$ . This coefficient is  $C_{\Delta}$  (equation (19)) on the

forward part of the wing and  $C_{\Delta} + (\Delta C)_{\circ} + \int_0^{a_{\circ}} \frac{d\Delta C}{da} da$  (see p. 8)

behind the trailing-edge Mach line. From Robinson's work, the longitudinal component of the suction force per unit length in the  $x$  direction may be expressed, for region I, in terms of  $C_{\Delta}$  as follows:

$$\frac{dT}{dx} = \frac{\rho\pi}{m} \sqrt{1-m^2} C_{\Delta}^2$$

and similarly for the remainder of the wing, with  $C_{\Delta}$  replaced by the corrected coefficient.

For a given wing, the total drag due to lift is the result of subtracting the total thrust from the product of the lift and the angle of attack; that is,

$$D = \alpha L - 2 \int_0^{\frac{\beta s}{m}} \frac{dT}{dx} dx \quad (39)$$

or, in coefficient form,

$$C_D = \frac{\alpha^2}{S} \left( \frac{L}{q\alpha} - \frac{2}{q\alpha^2} \int_0^{\frac{\beta s}{m}} \frac{dT}{dx} dx \right) \quad (40)$$

where  $S$  is the total area of the wing. Writing

$$\int_0^{\frac{\beta s}{m}} \frac{dT}{dx} dx = \frac{\rho\pi}{m} \sqrt{1-m^2} \left\{ \int_0^{x_1} C_{\Delta}^2 dx + \int_{x_1}^{\frac{\beta s}{m}} \left[ C_{\Delta} + (\Delta C)_0 + \int_0^{a_0} \frac{d\Delta C}{da} da \right]^2 dx \right\} \quad (41)$$

we obtain

$$\frac{2}{q\alpha^2} \int_0^{\frac{\beta s}{m}} \frac{dT}{dx} dx = \pi \sqrt{1-m^2} \left[ \left( \frac{u_0}{V\alpha} \right)^2 x_1^2 + \frac{4c_0}{m} \int_{x_1}^{\frac{\beta s}{m}} \sigma^2 dx \right] \quad (42)$$

so that

$$C_D = \frac{\alpha^2}{S} \left\{ \frac{L}{q\alpha} - \pi \sqrt{1-m^2} \left[ \left( \frac{u_0}{V\alpha} \right)^2 x_1^2 + \frac{4c_0}{m} \int_{x_1}^{\frac{\beta s}{m}} \sigma^2 dx \right] \right\} \quad (43)$$

with the final integration to be performed numerically or graphically.

## APPLICATION AND DISCUSSION

## Lift-Curve Slope

The lift-curve slope  $C_{L\alpha}$  has been calculated for two families of untapered wings, with  $m$  constant at 0.2 and 0.4, and with varying aspect ratio. The results are plotted against the reduced aspect ratio  $\beta A$  in figure 7. The circled points indicate the actual cases for which calculations were made; the faired curves are only approximations, since they ignore slight discontinuities in curvature associated with the onset of interaction between the wake and leading edge, and higher-order discontinuities associated with successive reflections of the trailing-edge Mach lines.

Two points corresponding to tapered wings with  $m = 0.4$  and  $m_t = 0.6$  are also included. In one case ( $\beta A = 1.6$ ), and in the case of the untapered wing with the same span ( $\beta A = 1.2$ ), the trailing-edge Mach lines did not intersect the leading-edge, and the values of  $C_{L\alpha}$  were obtained by the formulas of reference 1. It should also be mentioned that the remaining values agree within 2 or 3 percent with values calculated entirely by the conical-flows method, the former being slightly lower than the latter.

The curves for the untapered wings may be seen to be approaching at the upper end the value  $2\pi m / \sqrt{1-m^2}$  given by simple sweep theory. At the lower end, the curves should approach the origin along the line  $C_{L\alpha} = \frac{\pi}{2} A$  given by low-aspect-ratio theory (reference 14). As previously mentioned, the present calculations cannot properly be extended below  $\beta A = 1$  because of interference between the flow fields originating at the tips. However, two such cases have been included for  $m = 0.2$  because, with so much sweep, the wing areas affected are small and the interference losses should be negligible. Results in these latter cases may be compared, because of the small apex angle relative to the Mach angle, with the results of the slender-wing theory of reference 5. This comparison is shown in figure 7, although a discrepancy in plan form lessens the significance of the agreement.<sup>3</sup> The results of reference 5 have also been plotted for  $m = 0.4$ , in which case the assumption of extreme slenderness is no longer justified and introduces an appreciable error. (It should be mentioned that the asymptote for the slender-wing-theory curves is below the value given by simple sweep theory by the factor  $\sqrt{1-m^2}$ .)

---

<sup>3</sup>The theory of reference 5, while applicable to any swept-back wing lying well within the leading-edge Mach cone, has been worked out only for a limited family of plan forms, having straight leading and filleted trailing edges, and, consequently, a slight taper.

## Drag Due to Lift

In figure 8, the drag-rise factor  $C_D/C_L^2$  is plotted for the same families of wings. Comparison is made with a theoretical minimum for slender wings in supersonic flight obtained by R. T. Jones in an unpublished analysis. Using a method similar to Hayes' (reference 12) and assuming the wing to be narrow compared with the Mach cone, Jones has derived a minimum "wave drag" coefficient

$$C_{D_w} = \frac{\beta^2}{2\pi A_x} C_L^2 \quad (44)$$

where  $A_x$  is the aspect ratio defined in the streamwise, instead of the spanwise, direction; that is, if  $l$  (numerically equal to  $x_T$ ) is the over-all length of the wing,

$$A_x = l^2/S \quad (45)$$

The wave drag is to be added to the "vortex drag," which is the induced drag of subsonic flow, calculated from the spanwise loading. Using the minimum induced drag calculated from lifting-line theory gives as the minimum supersonic drag-rise factor

$$\frac{C_D}{C_L^2} = \frac{1}{\pi A} + \frac{\beta^2}{2\pi A_x} \quad (46)$$

It may be seen that the drag rise of the constant-chord swept-back wings is fairly close to the minimum, especially at the lower values of  $m$  for which equation (46) was derived.

Ames Aeronautical Laboratory,  
National Advisory Committee for Aeronautics,  
Moffett Field, Calif., Mar. 15, 1950.

## APPENDIX

## SYSTEM OF NOTATION

## General

V	free-stream velocity
M	free-stream Mach number
$\beta$	$\sqrt{M^2-1}$
$\rho$	density of air
q	dynamic pressure $\left(\frac{1}{2}\rho V^2\right)$
$\Delta p$	pressure difference between upper and lower surfaces, or local lift
$\alpha$	angle of attack, radians
L	lift
$C_L$	lift coefficient $\left(\frac{L}{qS}\right)$
$C_D$	drag coefficient $\left(\frac{D}{qS}\right)$

## Wing Dimensions

$c_o$	root chord
$c_t$	tip chord
s	semispan
S	wing area
l	over-all length of the wing in the streamwise direction
$\Lambda$	angle of sweep of the leading edge
$\lambda$	taper ratio ( $c_t/c_o$ )

A aspect ratio ( $4s^2/S$ )

### Coordinates

$x, y$  Cartesian coordinates in the stream direction and across the stream in the plane of the wing

$x_a, y_a$  coordinates of apex of oblique trailing-edge element (see equation (14))

$x_b, y_b$  coordinates of point on trailing edge, within the tip-Mach cone

$x_c, s$  coordinates of point on tip; apex of tip element

$x_1, y_1$  coordinates of intersection of trailing-edge Mach cone with leading edge (see equation (11))

$x_2, y_2$  coordinates of intersection of Mach line from  $x_1, y_1$  with trailing edge (see equation (13))

$x^*, y^*$  coordinates of intersection of tip Mach line with trailing edge

$x_T, s$  coordinates of intersection of tip and trailing edge

$\xi^*$  streamwise distance of  $x^*, y^*$  back from leading edge, as a fraction of the tip chord (equation (37))

$\xi_c$  distance of  $x_c$  behind leading-edge tip, as a fraction of the tip chord (equation (29))

In the following, all slopes are measured counterclockwise from a line extending downstream from the apex of the wing or of the pertinent elementary sector:

$$m \quad \frac{\text{slope of leading edge}}{\text{slope of Mach lines}} = \beta \cot \Lambda$$

$$m_t \quad \frac{\text{slope of trailing edge}}{\text{slope of Mach lines}}$$

$$a \quad \frac{\text{slope of ray from the origin}}{\text{slope of Mach lines}} = \beta \frac{y}{x}$$

$$t_o \quad \frac{\text{slope of ray from trailing-edge apex}}{\text{slope of Mach lines}} = \beta \frac{y}{x-c_o}$$



$$t_m \frac{\text{slope of ray from leading-edge tip}}{\text{slope of Mach lines}} = \beta \frac{y-s}{x-\frac{\beta s}{m}}$$

$$t_a \frac{\text{slope of ray from apex of element } a}{\text{slope of Mach lines}} = \beta \frac{y-y_a}{x-x_a}$$

$$t_c \frac{\text{slope of ray from apex of tip element}}{\text{slope of Mach lines}} = \beta \frac{y-s}{x-x_c}$$

$a_0$  the value of  $a$  corresponding to a trailing-edge element of which the apex lies on the Mach forecone of the point at which the load is being calculated (equation (22))

$a_2$   $a(x_2, y_2)$  (equation (8))

$\tau_0$  the smallest value of  $t_0$  along which cancellation of pressure ahead of the leading edge can affect the point at which pressure is being calculated. For a point on the leading edge,  
 $\tau_0 = t_0 = mx/(x-c_0)$

$\tau_a$  the smallest values of  $t_a$  along which cancellation of pressure ahead of the leading edge can affect the point at which pressure is being calculated. For a point on the leading edge,  
 $\tau_a = t_a = (mx - \beta y_a)/(x - x_a)$

#### Streamwise Components of Perturbation Velocity

$u_\Delta$  basic (uncorrected) perturbation velocity as given by solution for triangular wing (equation (1))

$u_0$  value of  $u_\Delta$  at  $a=0$  (equation (2))

$u_a$  constant perturbation velocity on canceling (oblique) sector in wake (equation (6))

$u_c$  constant perturbation velocity on canceling sector outboard of tip

$(\Delta u)_0$  symmetrical trailing-edge correction to  $u_\Delta$  (equation (3))

$(\Delta u)_a$   $\frac{d\Delta u}{da} da$ , correction to  $u_\Delta$  due to single oblique trailing-edge element (equation (5))

$\Delta u^*$  value of tip correction to  $u$  at the point  $x^*, y^*$  (equation (36))

## Arbitrary Mathematical Symbols

- $C_{\Delta}$  value of coefficient of  $(mx-\beta y)^{-1/2}$  in  $u_{\Delta}$  at the leading edge (equation (19))
- $(\Delta C)_{\circ}$  decrement in  $C_{\Delta}$  due to reflection of  $(\Delta u)_{\circ}$  at leading edge (equation (20))
- $\frac{d\Delta C}{da}$  da decrement in  $C_{\Delta}$  due to reflection of  $(\Delta u)_{\text{a}}$  at leading edge (equation (21))
- $\sigma$  leading-edge correction coefficient defined by equation (17)
- $\sigma_{\text{S}}$  value of  $\sigma$  at leading-edge tip

## Elliptic Integrals

- $k$  modulus of elliptic integral, defined where used (also with subscripts)
- $\varphi$  or  $\psi$  argument of elliptic integrals, defined where used (also with subscripts)
- $F(k, \varphi)$  incomplete elliptic integral of the first kind of modulus  $k$  and argument  $\varphi$
- $K, K(k)$  complete elliptic integral of the first kind of modulus  $k$ ; that is,  $K = F(k, \frac{\pi}{2})$
- $E(k, \varphi)$  incomplete elliptic integral of the second kind
- $E, E(k)$  complete elliptic integral of the second kind of modulus  $k$ ;  
 $E(k, \frac{\pi}{2})$

## REFERENCES

1. Lagerstrom, P. A., Wall, D. D., and Graham, M. E.: Formulas in Three-Dimensional Wing Theory. Douglas Rep. SM-11901, Aug. 1946.
2. Cohen, Doris: The Theoretical Lift of Flat Swept-Back Wings at Supersonic Speeds. NACA TN 1555, 1948.

3. Malvestuto, Frank S., Jr., Margolis, Kenneth, and Ribner, H. S.: Theoretical Lift and Damping in Roll of Thin Sweptback Wings of Arbitrary Taper and Sweep at Supersonic Speeds. Subsonic Leading Edges and Supersonic Trailing Edges. NACA TN 1860, 1949.
4. Cohen, Doris: Theoretical Loading at Supersonic Speeds of Flat Swept-Back Wings with Interacting Trailing and Leading Edges. NACA TN 1991, 1949.
5. Lomax, Harvard, and Heaslet, Max. A.: Linearized Lifting-Surface Theory for Swept-Back Wings with Slender Plan Forms. NACA TN 1992, 1949.
6. Jones, R. T.: Estimated Lift-Drag Ratios at Supersonic Speed. NACA TN 1350, 1947.
7. Hayes, W. D., Browne, S. H., and Lew, R. J.: Linearized Theory of Conical Supersonic Flow with Application to Triangular Wings. North American Aviation Rep. NA-46-818, Sept. 30, 1946.
8. Squire, H. B.: An Example in Wing Theory at Supersonic Speeds. Abstract in Proceedings of the Seventh International Congress for Applied Mechanics, 1948. vol. 2, Part II, p. 614.
9. Lagerstrom, P. A.: Linearized Supersonic Theory of Conical Wings. NACA TN 1685, 1948.
10. Busemann, A.: Infinitesimal Conical Supersonic Flow. NACA TM 1100, 1947.
11. Betz, A.: Applied Airfoil Theory. Vol. IV, div. J of Aerodynamic Theory, W. F. Durand, ed., Julius Springer (Berlin) 1935. p. 28.
12. Hayes, W. D.: Linearized Supersonic Flow. North American Aviation, Inc., Rep. no. AL-222, June 18, 1947.
13. Jones, R. T.: Leading-Edge Singularities in Thin Airfoil Theory. Jour. Aero. Sci., vol. 17, no. 5, May 1950, pp. 307-310.
14. Jones, R. T.: Properties of Low-Aspect-Ratio Pointed Wings at Speeds Below and Above the Speed of Sound. NACA Rep. 835, 1946.

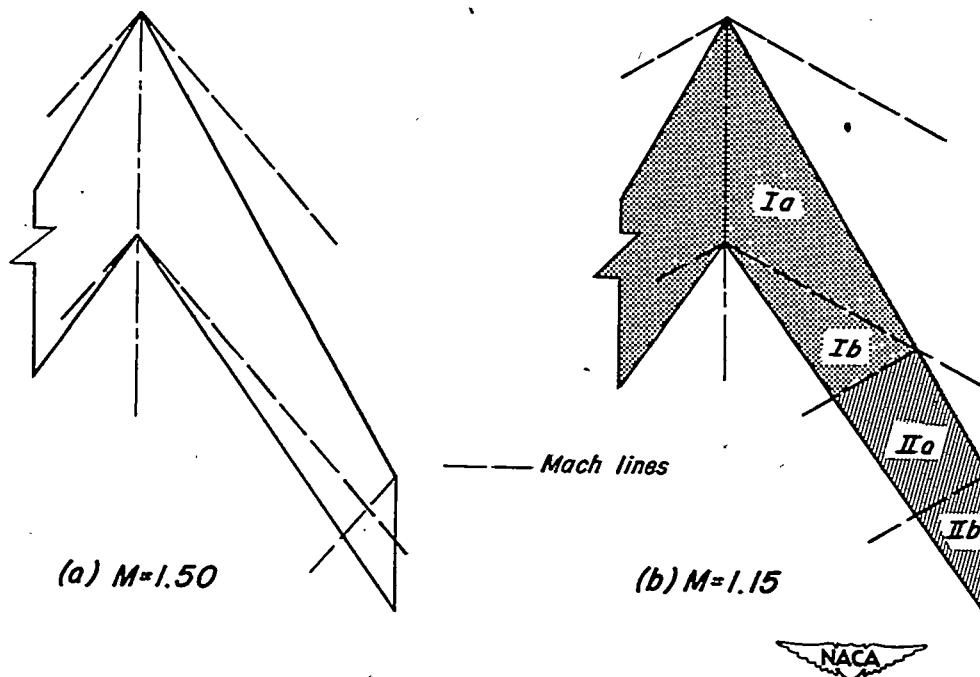


Figure 1.- Plan view of swept-back wing at two supersonic Mach numbers.

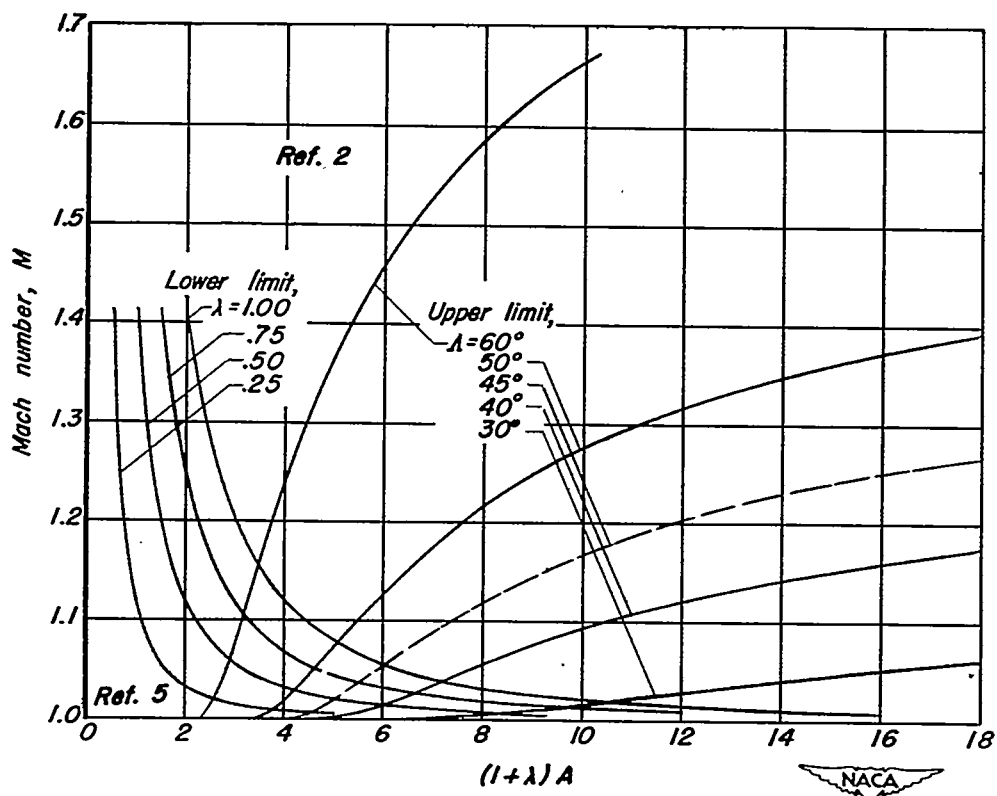


Figure 2.- Range of applicability of formulas and charts.

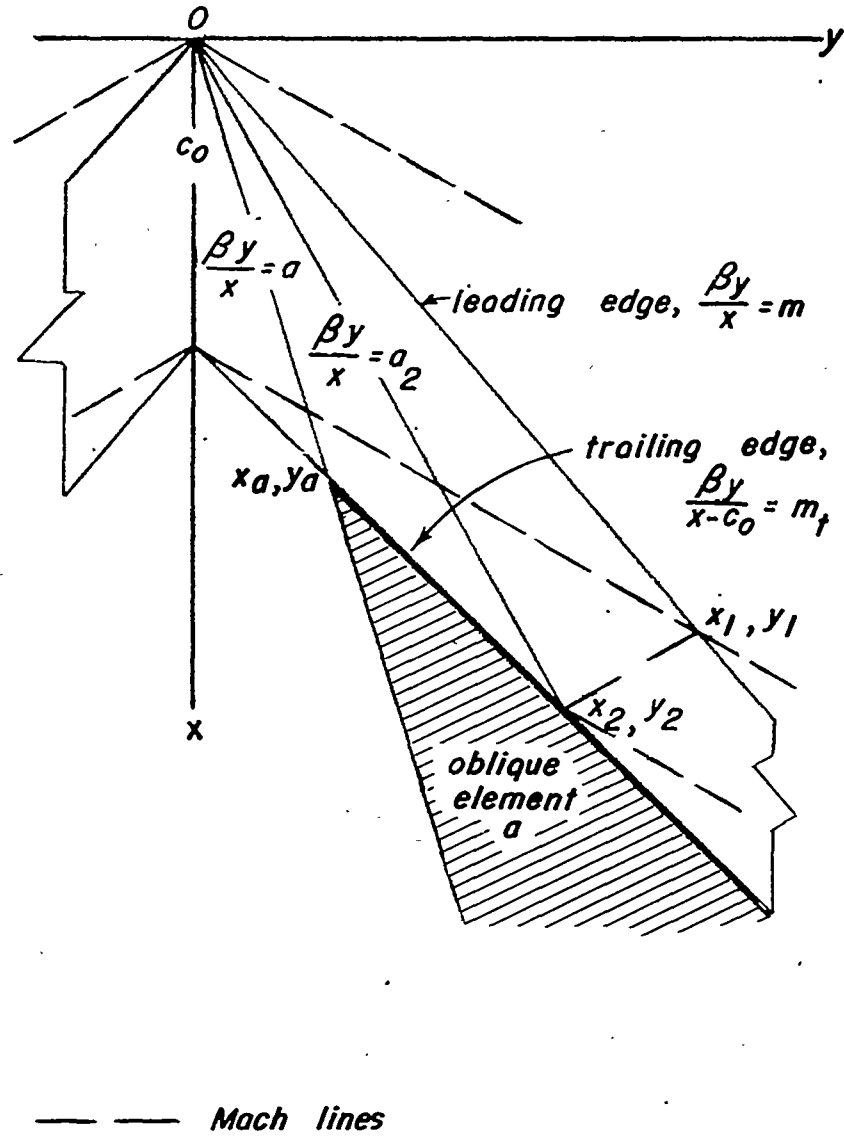


Figure 3.- Coordinate System and other Symbols.

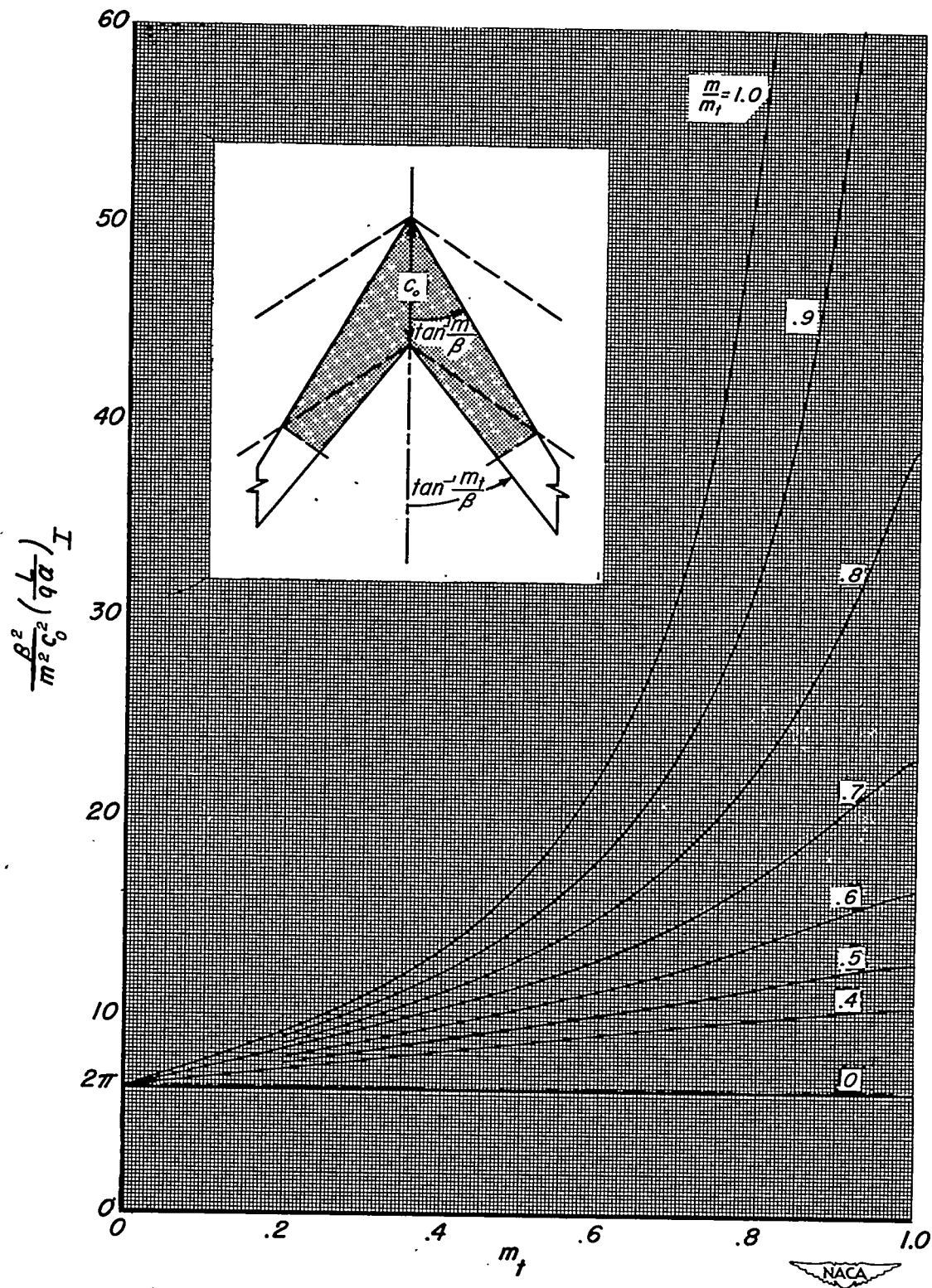


Figure 4.- Chart for the computation of the lift in region I.

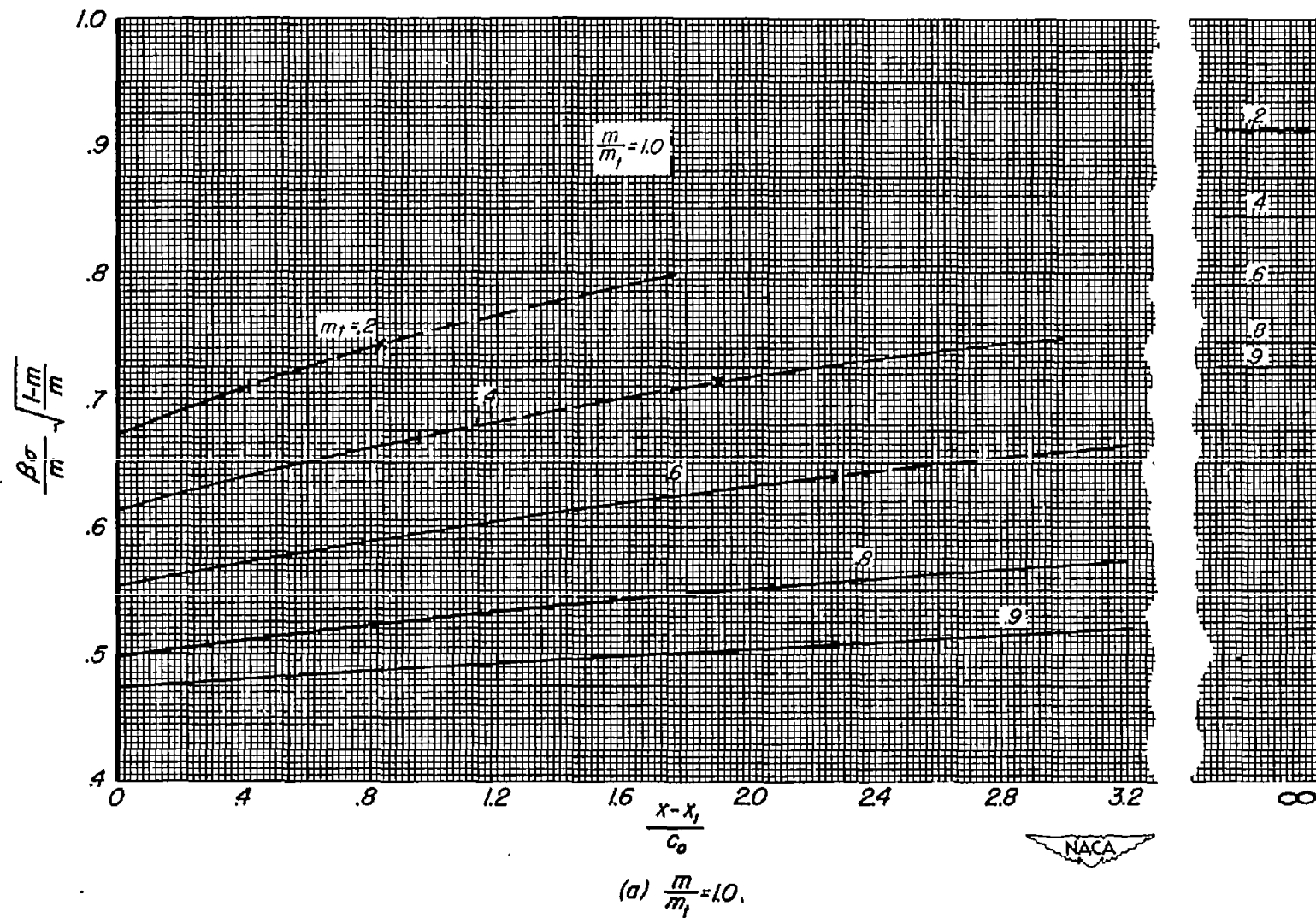
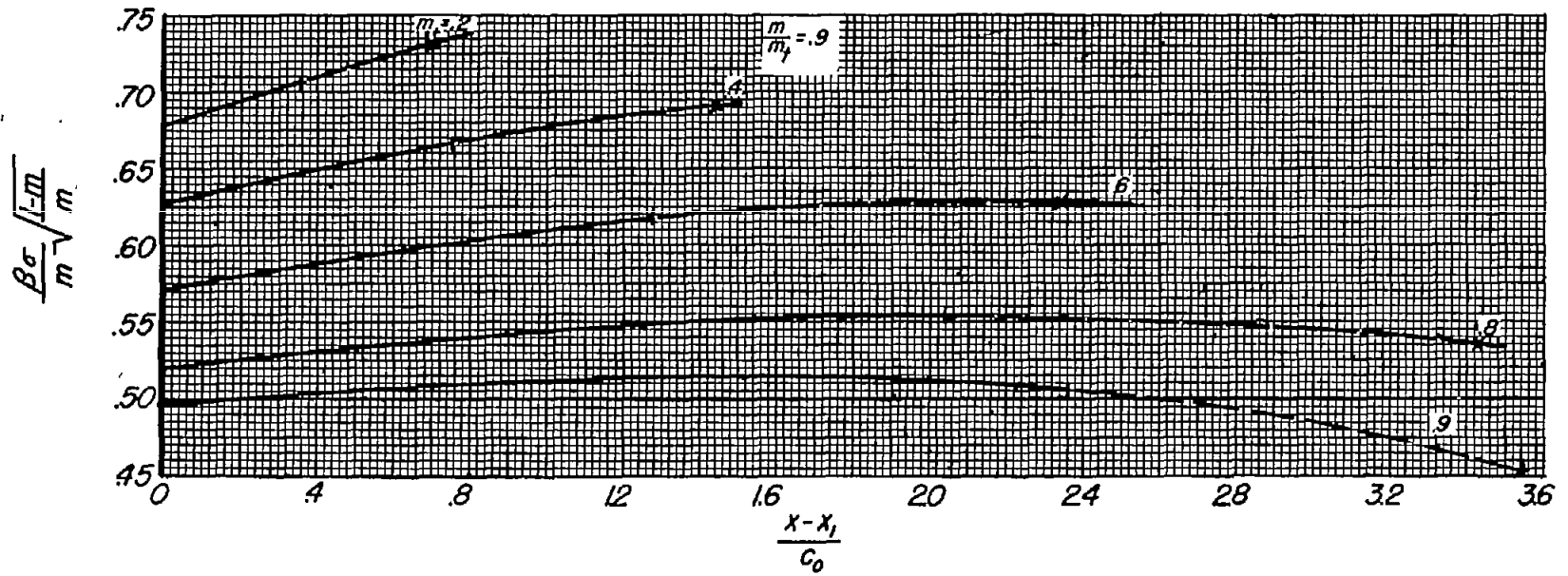


Figure 5.— Charts for determining  $\sigma$ , the strength of the leading-edge singularity.

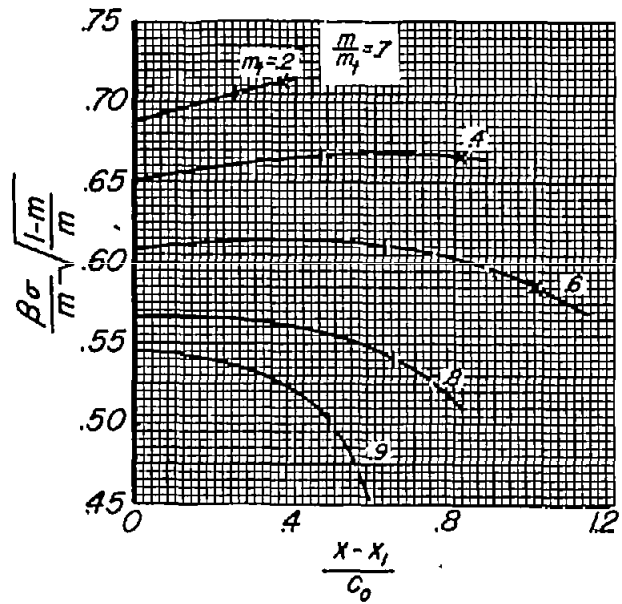
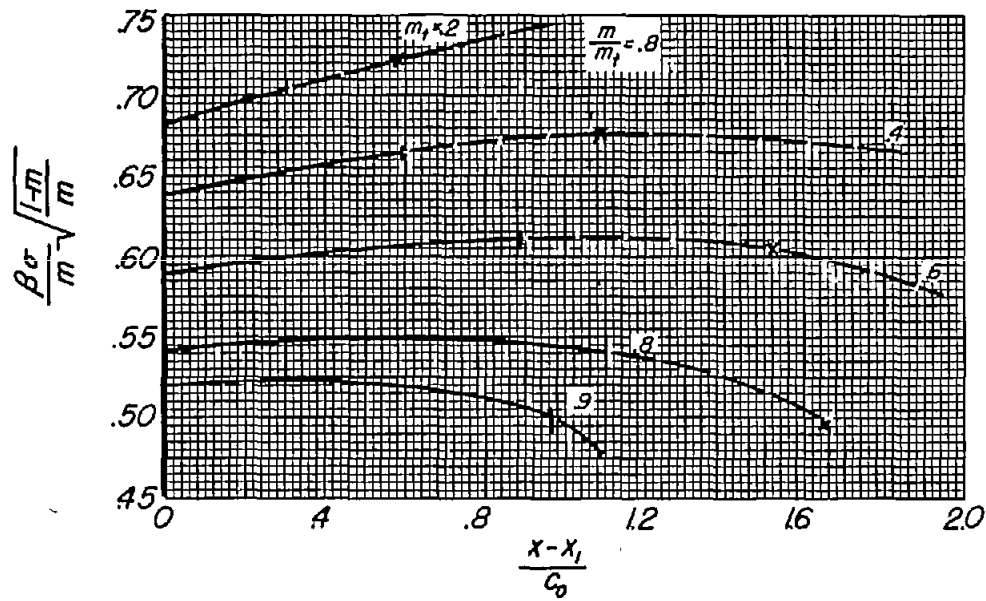


(b)  $\frac{m}{m_1} = .9$ .



Figure 5.- Continued.

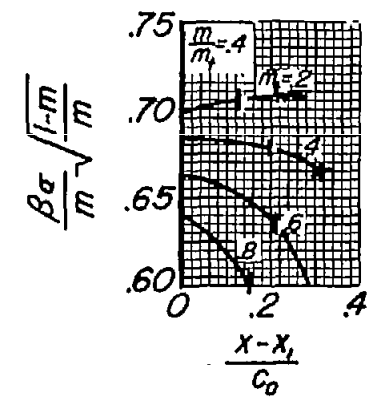
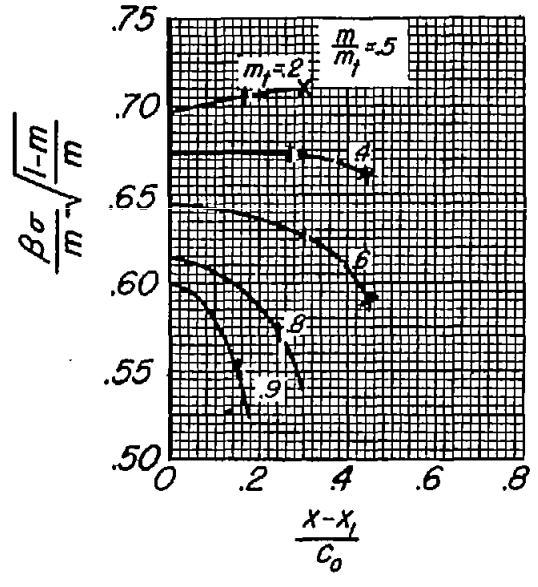
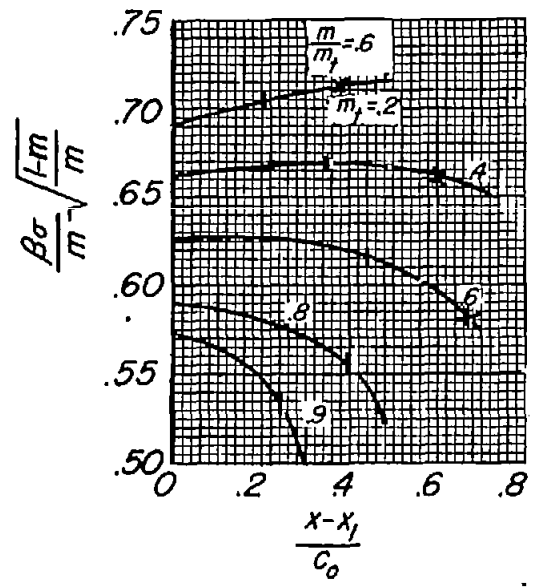




(c)  $\frac{m}{m_1} = .8$  and  $.7$ .



Figure 5.- Continued.



(d)  $\frac{m}{m_1} = .6, .5, \text{ and } 4.$



Figure 5.- Concluded.

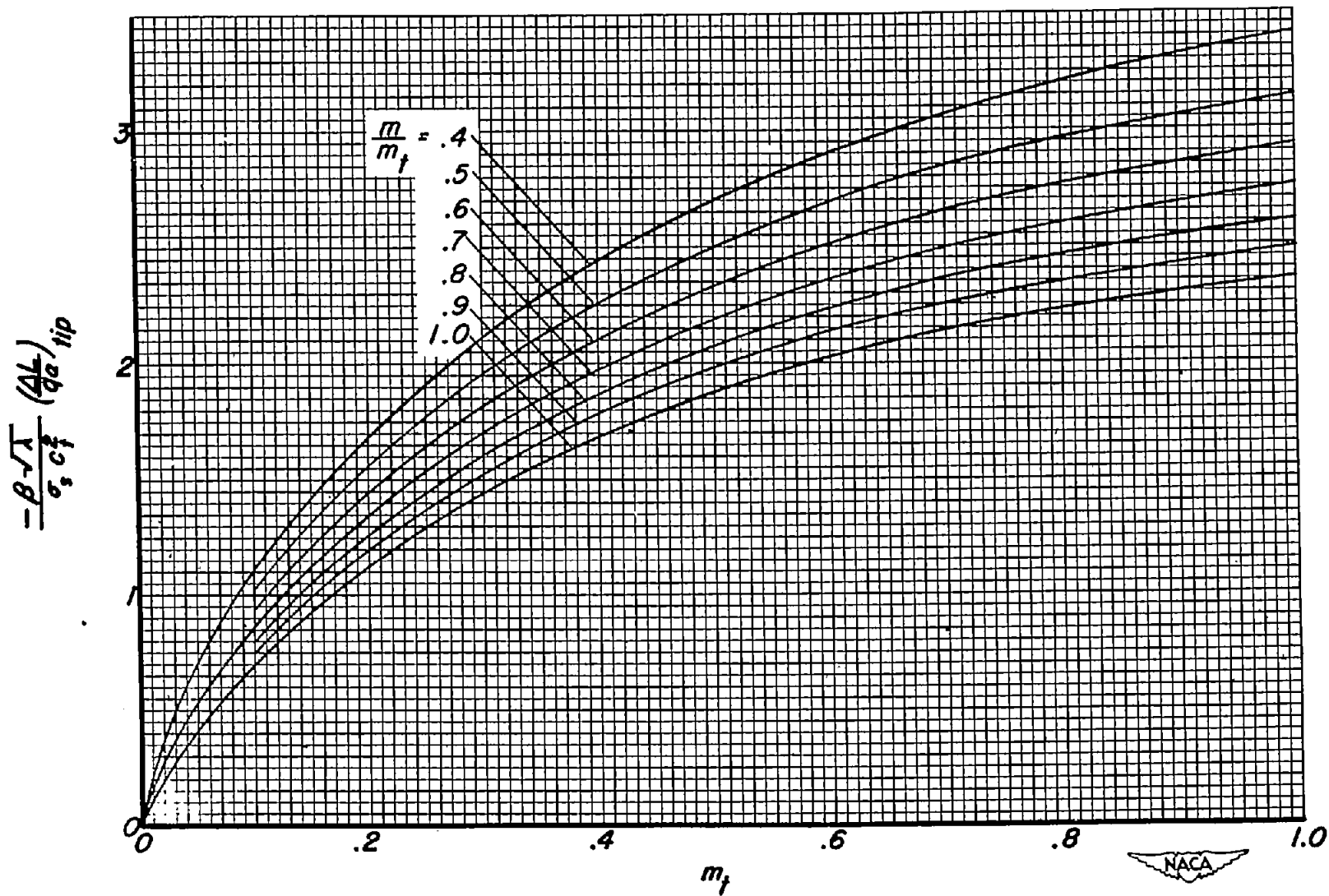


Figure 6.- Chart for the correction of the lift for tip effect.

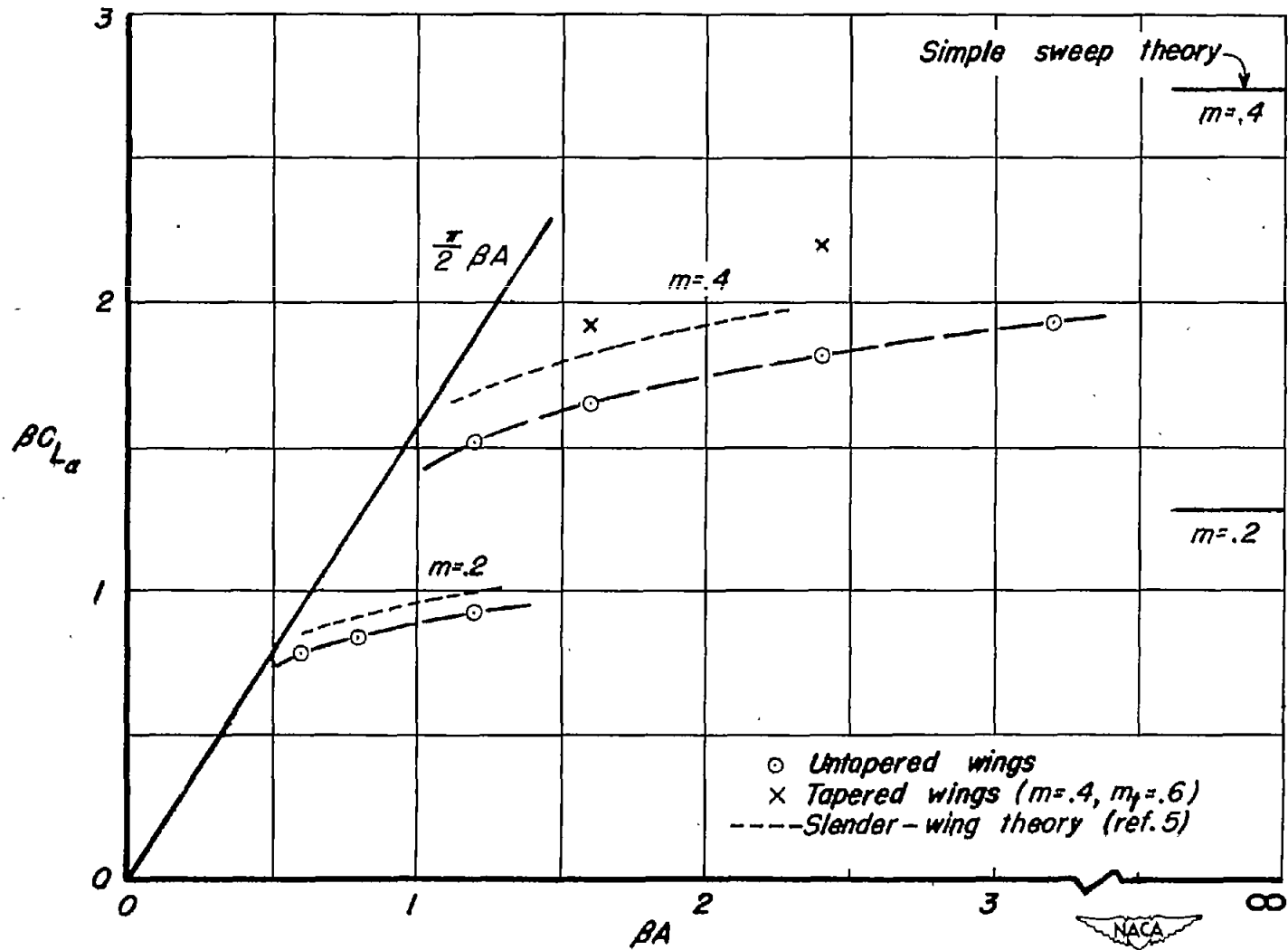


Figure 7.- Variation of lift-curve slope with aspect ratio.

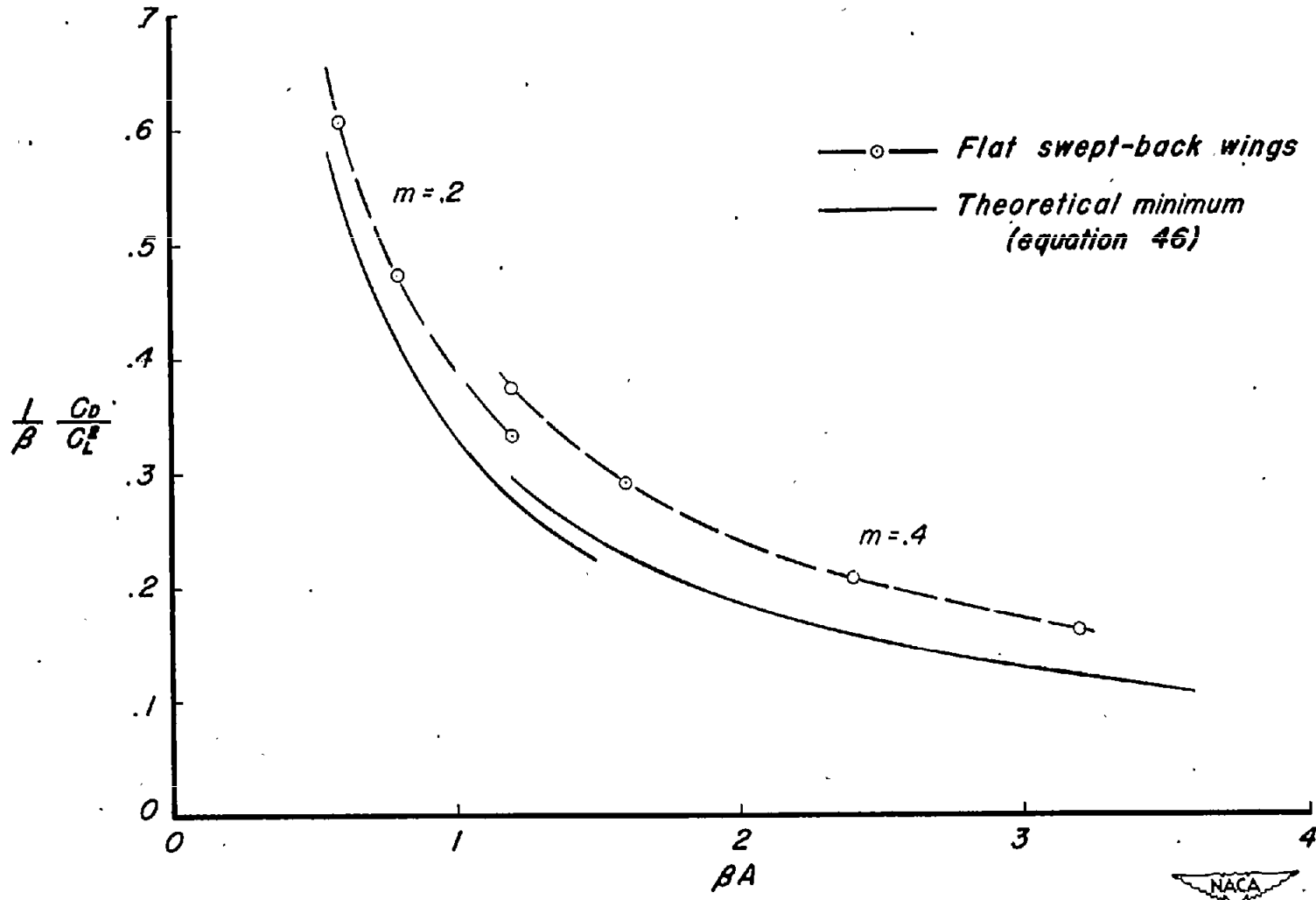


Figure 8.- Drag-rise factor  $\frac{C_d}{C_{d0}}$  for untapered wings.

